

## Defect structure in micropillars using x-ray microdiffraction

R. Maaß, D. Grolimund, S. Van Petegem, M. Willmann,  
M. Jensen, and H. Van Swygenhoven<sup>a)</sup>  
*Paul Scherrer Institute, CH-5232 Villigen, Switzerland*

T. Lehnert and M. A. M. Gijs  
*Ecole Polytechnique Fédérale de Lausanne, Institute of Microelectronics and Microsystems,  
CH-1015 Lausanne, Switzerland*

C. A. Volkert, E. T. Lilleodden, and R. Schwaiger  
*Institut für Materialforschung-II, Forschungszentrum Karlsruhe, D-76021 Karlsruhe, Germany*

(Received 27 June 2006; accepted 10 August 2006; published online 11 October 2006)

White beam x-ray microdiffraction is used to investigate the microstructure of micron-sized Si, Au, and Al pillars fabricated by focused ion beam (FIB) machining. Comparison with a Laue pattern obtained from a Si pillar made by reactive ion etching reveals that the FIB damages the Si structure. The Laue reflections obtained from the metallic pillars fabricated by FIB show continuous and discontinuous streakings, demonstrating the presence of strain gradients. © 2006 American Institute of Physics. [DOI: 10.1063/1.2358204]

Size effects in plasticity resulting from the reduction in specimen size have received much attention in recent years since conventional theories do not explicitly incorporate geometrical length-scale dependencies. In order to circumvent the coupled effects of strain gradients, as are encountered in nanoindentation and wafer curvature testing, microcompression testing is a technique to study the effects of geometric size.<sup>1-4</sup> In these experiments, a columnar structure is fabricated, typically using focused ion beam (FIB) machining from a thin film or bulk specimen, with diameters on the order of tens of microns down to 100 nm. The columns are then compressed using a nanoindenter outfitted with a flat punch indenter. The results show a general trend of increasing strength with decreasing diameters. The rationale for such behavior is greatly debated, with emerging theories including dislocation exhaustion and stochastic, scale-free dislocation mechanisms.<sup>2,3,5,6</sup>

Computational simulations are currently being carried out in order to explore the origin of this geometric length-scale size effect. Recent results from a dislocation dynamics simulation utilizing a homogeneous distribution of Frank-Read sources have reproduced the experimental observation that smaller is stronger in both two dimensional<sup>7,8</sup> and three dimensional<sup>9</sup> simulations. However, these results may be fortuitous if the initial microstructure used in the simulation does not appropriately represent the sample. Such characterization of the initial structure is critical to understand the underlying mechanisms of the observed size effects. However, experimental difficulties have limited internal structure characterization of columns prior to deformation. Nondestructive methods with high spatial resolution are required; characterization of adjacent material from which the column is fabricated may not be appropriate, due to spatial variation in defect distribution, and more importantly, due to potential artifacts caused by the column fabrication process itself. The latter is of particular concern for FIB machined structures. Although it is believed that Ga implantation has a minor effect on the initial microstructure of metallic structures,<sup>1</sup> the

implanted ions create highly mobile point defects that can collapse in planar defect structures. For example, careful studies of FIB and conventionally electropolished Cu-based transmission electron microscopy samples have demonstrated a significant increase in dislocation density in the FIB samples.<sup>10</sup>

To shed light on the initial microstructure and on possible FIB damage we have performed polychromatic Laue diffraction at the microXAS beamline of the Swiss Light Source on Si pillars made both by FIB milling and by deep reactive ion etching (DRIE, SF<sub>6</sub> plasma for etching, C<sub>4</sub>F<sub>8</sub> for passivation) and on Au and Al pillars made by FIB milling. The DRIE process is optimized for smooth sidewalls. Further sidewall smoothing was obtained by oxidizing the pillar with a 0.5 μm thick sacrificial layer which was subsequently removed by wet etching. The DRIE prepared Si pillar has a diameter of about 1 μm and a height of 2.6 μm. The FIB prepared pillars were made by perpendicular FIB milling (30 keV, final polishing step with 50 pA)<sup>3</sup> of either patterned single crystal (100) Si wafers, large grain Au wire, or slices of polycrystalline Al films on Si. The 4 μm diameter Au and the 2.7 μm diameter Si were single crystal and the 4 μm diameter Al pillar contained around six grains. Pt markers were deposited by FIB in the neighborhood of the pillars to facilitate alignment in the x-ray beam.

Polychromatic diffraction patterns were performed in conventional Laue transmission geometry with photon energies ranging from 2 to 20 keV. Kirkpatrick-Baez mirror focusing optics was used to obtain a beam full width at half maximum of 3 × 4 μm<sup>2</sup> in the focal plane with a maximum angular divergence of 0.2 × 0.3 mrad. The sample pillars were mounted perpendicular to the beam at the focal plane using a four-axis sample manipulator with submicron positioning accuracy. Fluorescent signal mappings of the Pt markers (for the Si and Al samples) and of the Au were used to locate the pillars and ensure full illumination while avoiding irradiation of the underlying material. A large area charged-coupled-device (CCD) detector with 3862 × 2526 pixel resolution and a pixel size of 32 μm<sup>2</sup> recorded the diffraction patterns at a sample to detector distance of

<sup>a)</sup>Electronic mail: helena.vanswygenhoven@psi.ch

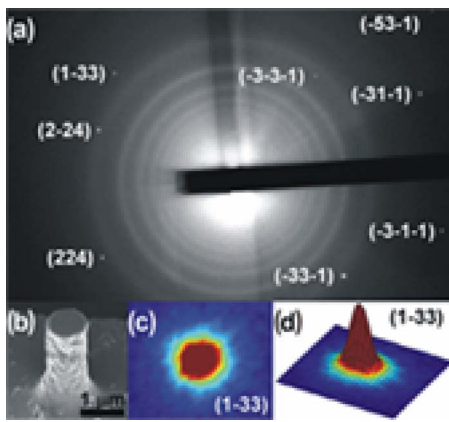


FIG. 1. (Color online) Laue pattern of DRIE-Si pillar (a), SEM picture (b), truncated contour plot (c), and 2D intensity distribution (d) of (1-33).

53.5 mm. The CCD plate was placed perpendicular to the incident beam direction, which, combined with the relative low energy range of the beam, resulted in a limited number of reflections that could be recorded.

The Laue patterns of the Si pillars show reflections from the (331), (113), and (242) families of lattice planes for the incoming beam parallel to the [011] direction. Figure 1 shows results for the DRIE-Si pillar, including a Laue pattern (a), a scanning electron microscope (SEM) image of the pillar (b), the truncated contour plot (c), and two dimensional (2D) intensity profile (d) of the (1-33) Laue reflection. All reflections show peak shapes similar to the peak profiles of a Si wafer reference sample. The observed asymmetry in the 2D intensity plot (d) is therefore a result of the beam divergence profile, the scattering, and the detector geometry. The rings visible in the background of the Laue pattern have a very low intensity (intensities of peak/ring/background are 5000/250/200) and are probably due to a surface oxide layer on the pillar.

The Laue pattern of the FIB-Si pillar is similar to that from the DRIE-Si pillar and shows nine reflections of the same families. Figure 2 shows a SEM picture of the FIB-Si pillar and the contour plots of the (1-33), (133), and (113) reflections. Laue spot streaking was observed for all recorded reflections; however, the profile of the intense part of the peak was similar to the one observed for the DRIE-Si pillar. The streaking direction is peak dependent as can be seen in

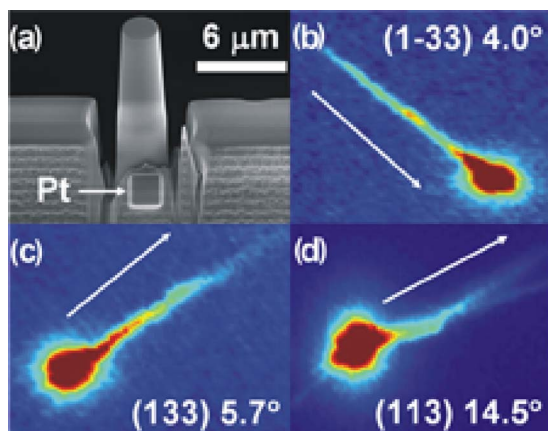


FIG. 2. (Color online) SEM picture of the FIB-Si pillar (a) and contour plots of the reflections [(b)-(d)] (1-33), (133), and (113).

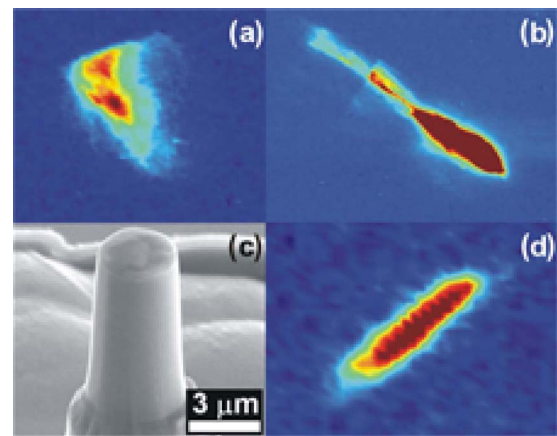


FIG. 3. (Color online) Contour plots of two reflections of the Au pillar [(a) and (b)], SEM picture of the Al pillar (c), and contour plot of an Al reflection showing continuous streaking (d).

Fig. 2 where the arrow on the contour plots points towards the center of the Laue pattern and the angle given in degrees gives the offset from the radial direction. The intensity of the streaks is low compared to the intensity of the main diffraction peaks for all observed reflections from the FIB-Si, suggesting that the volume of the damaged region causing the streaking is small.

The white beam Laue pattern of the Au pillar contains four heavily streaked and asymmetric reflection peaks. Due to the fact that the initial orientation of the pillar is not known, the pattern with very few diffraction spots could not be indexed. Figures 3(a) and 3(b) show representative contour plots of two of the reflections observed for the Au pillar. Both reflections show discontinuous intensity distributions, where (a) shows peak splitting in both radial and azimuthal directions of the Laue pattern by  $0.26^\circ$  and  $0.3^\circ$ , respectively, with both subpeaks having about equal intensities, whereas (b) shows the presence of splitting predominantly in the radial direction. The Al pillar, shown in Fig. 3(c), shows a higher number of Laue reflections due to the fact that it contains approximately six grains. Some of the reflections show similar discontinuous intensity distributions whereas others show large, continuous streaking as demonstrated in Fig. 3(d).

White beam Laue diffraction patterns taken from either perfect single crystals or from single crystals containing randomly distributed dislocations with no net Burgers vector content<sup>11-13</sup> exhibit uniform, axisymmetric peaks (assuming effects from thermal asterism are negligible). However, the presence of an excess of dislocations of one type (unpaired dislocations) or the presence of dislocation patterns can lead to strong nonaxisymmetric peak broadening and continuous or discontinuous Laue streaking.<sup>13</sup> For instance, unpaired geometrically necessary boundary dislocations cause discontinuous streaking while unpaired geometrically necessary individual dislocations would cause continuous streaking.<sup>12</sup> The streak direction of the Laue spot depends on the dislocation tensor and the effective strain gradient. In the case of single slip the streak direction depends on the dislocation slip system orientation. Inhomogeneous deviatoric elastic strains can also cause Laue streaking provided the elastic strains are large enough.

The comparison of the FIB prepared and etched Si pillars clearly illustrates that the FIB introduces damage in the

Si. For the DRIE-Si pillar the peak profiles can be explained by the beam divergence of the x-ray microbeam. The low intensity Laue streaking observed for the FIB-Si pillar must then be related to a small volume of material that is damaged by FIB milling. It is well known that FIB milling of Si creates a surface amorphous layer,<sup>14</sup> as well as Ga incorporation, which could lead to a complex strain distribution within the pillar.<sup>15</sup> The observed amount of streaking could be explained by anisotropic elastic strain distributions within the pillar, but to rule out contributions of excess dislocations or pure rotational effects due to, for instance, recrystallization of an amorphous layer,<sup>14</sup> further investigations are needed.

The asymmetric intensity distributions from the FIB-Au and FIB-Al pillars are much more significant than those from the FIB-Si. The high intensities of the streaks and splitting of the peaks in the Laue patterns indicate contributions from large fractions of the pillar volumes. According to current understanding of streaking in Laue patterns, the results indicate that the FIB-metal pillars not only contain unpaired dislocations in the lattice but also rotational displacement fields<sup>11-13</sup> and possibly dilatational effects, the latter needing energy scans for confirmation.<sup>16</sup> It is well known that FIB does introduce structural defects such as dislocations<sup>10</sup> in soft fcc metals, and therefore it can be expected that part of the microstructure we are observing results from making the pillars. However, to what extent the structure is due to FIB treatment and is different from the starting material are matters for further research.

In summary, the current results demonstrate the power of white beam Laue diffraction to contribute to the understanding of size effects in plasticity and how it relates to the initial microstructure of micropillars. The above results demonstrate that at least for Si the sample preparation does interfere with the initial microstructure. Our observations on Al and Au pillars show that the initial microstructure is more complex than a simple homogeneous distribution of dislocations with no net Burgers vector content, demonstrating the presence of strain gradients in micropillars. Knowledge of the

initial dislocation structure is essential as input for mesoscopic simulations such as dislocation dynamics that aim to understand size effects in plasticity, a topic that currently receives intense international focus.

The authors thank the EPFL Center of MicroNano Technology (EPFL-CMI) for help in the process development, in particular, Michaël Pavius for preparing the FIB samples; furthermore the authors thank Stefan Brandstetter for help during beam time and Peter M. Derlet for useful discussions. One of the authors (H.V.S.) thanks the Swiss National Science Foundation and the European Commission (sixth Framework) for financial support of the project NANOMESO.

<sup>1</sup>M. D. Uchic, D. M. Dimiduk, J. N. Florando, and W. D. Nix, *Science* **306**, 5699 (2004).

<sup>2</sup>J. R. Greer, W. C. Oliver, and W. D. Nix, *Acta Mater.* **53**, 1821 (2005).

<sup>3</sup>C. A. Volkert and E. T. Lilleodden, *Philos. Mag.* (in press).

<sup>4</sup>M. D. Uchic and D. M. Dimiduk, *Mater. Sci. Eng., A* **400-401**, 268 (2005).

<sup>5</sup>D. M. Dimiduk, M. D. Uchic, and T. A. Parthasarathy, *Acta Mater.* **53**, 4065 (2005).

<sup>6</sup>D. M. Dimiduk, C. Woodward, R. Lesar, and D. M. Uchic, *Science* **312**, 5777 (2006).

<sup>7</sup>V. S. Deshpande, A. Needleman, and E. van der Giessen, *J. Mech. Phys. Solids* **53**, 2661 (2005).

<sup>8</sup>A. A. Benzerga and N. F. Shaver, *Scr. Mater.* **54**, 1937 (2006).

<sup>9</sup>D. Weygand, M. Pognant, P. Gumbsch, and O. Kraft, *Mater. Sci. Eng., A* (to be published).

<sup>10</sup>C. R. Hutchinson, R. E. Hackenberg, and G. J. Shiflet, *Ultramicroscopy* **94**, 37 (2003).

<sup>11</sup>R. I. Barabash, *Mater. Sci. Eng., A* **309-310**, 49 (2001).

<sup>12</sup>R. I. Barabash and G. E. Ice, *Microdiffraction Analysis of Hierarchical Dislocation Organization*, Encyclopedia of Materials Science: Science and Technology Updates (Elsevier, Oxford, 2005), pp. 1-18.

<sup>13</sup>W. Yang, B. C. Larson, G. M. Pharr, G. E. Ice, J. D. Budai, J. Z. Tischler, and W. Liu, *J. Mater. Res.* **19**, 66 (2004).

<sup>14</sup>S. Rubanov and P. R. Munroe, *J. Microsc.* **214**, 213 (2004).

<sup>15</sup>C. A. Volkert, *J. Appl. Phys.* **70**, 3521 (1991).

<sup>16</sup>R. Barabash, G. E. Ice, B. C. Larson, G. M. Pharr, K.-S. Chung, and W. Yang, *Appl. Phys. Lett.* **79**, 749 (2001).